Application of internal multiple prediction: from synthetic to lab to land data

Melissa Hernandez and Kris Innanen

ABSTRACT

Multiple reflections represent a serious problem in the field of seismic processing. Multiple events can be mistaken for primary reflections, and may distort primary events and obscure the task of interpretation. In this work we will focus in the prediction of internal multiples and we will illustrate how the inverse scattering internal multiple algorithm introduced by Weglein and Araujo in 1994, is capable to attenuate internal multiples without any a priori information about the medium through which the waves propagate. One of the advantages of this method over other is its ability to suppress multiples that interfere with primaries without attenuating the primaries themselves. I consider the version of the algorithm for 1D normal incidence case.

In this work we promote a stepped approach to predicting multiples in a given field data set: first, by carrying out synthetic/numerical examples; second by carrying out tests on laboratory physical modeling data; and finally by testing prediction of a field data set suspected to be strongly contaminated with internal multiples.

INTRODUCTION

For the exploration of oil and gas reservoirs, multiples can be one of the main issues in applying the seismic method. The inverse scattering series internal multiple (Araujo et al., 1994) attenuation method is capable of attenuating internal multiples without any a priori information about the medium through which the waves propagate, i.e., is a data-driving process. Furthermore, the primaries reflections remain untouched. The output of the algorithm is a data set that contains the predicted multiples.

Every event in the seismic record can be thought of as a group of subevents. This algorithm predicts an internal multiple from interpreted subevents by performing a convolution and a crosscorrelation of the data. One of the most important characteristic of this algorithm is that it selects all the subevents that suit the lower-higher-lower relation (Weglein et. al., 1998). The parameter epsilon limits the selection or searching of the subevents and is related to the source wavelet. The inverse scattering attenuation method has three basics assumptions in order to work properly: knowledge of the source wavelet within the seismic frequency band, the input data must be free surface multiple, and accomplishment of pseudo depth condition lower-higher-lower.

The first term in the internal multiple attenuation series for the 1D normal incidence case is (Araujo et. al. 1994):

$$b_{3IM}(k_z) = \int_{-\infty}^{\infty} dz'_1 \; e^{k_z i\, z'_1}\, b_1(z'_1). \int_{-\infty}^{z'_1-\epsilon} dz'_2 b_1(z'_2). e^{-ik_z z'_2} \int_{z'_2+\epsilon}^{\infty} dz'_3 b_1(z'_3). e^{ik_z z'_3} \quad (1)$$

Here k_z and z are de pseudo depth wavenumber and pseudo depth ($z=c_o t/2$) respectively. The equation above predict the travel time of the first order internal multiples and approximate their amplitude.

The parameter epsilon (ϵ) ensures that z'_1 is always greater than and not equal to z'_2 and similarly for z'_3. This parameter is related to the width of the wavelet, and could be estimated knowing the source wavelet or an approximation.

The b_1 function is the seismic data after a series of transformations. In order to obtain b_1 we begin with the measured surface data with no free-surface multiples, $D(x_g, x_s, t)$ where x_g and x_s are the receiver location, source location and time respectively. Then, $D(k_g, k_s, \omega)$ is obtained by performing of 3D Fourier Transform on these data. Subsequently, the data is transformed to vertical wave number, $D(k_g, k_s, q_g+q_s)$. The third step is to transform the data to pseudo-depth establishing that $k_z = q_g+q_s$. Then, the inverse Fourier Transform is performed to the data, $b_1(k_g, k_s, k_z)$ to $b_1(k_g, k_s, z)$. Pseudo depth is an axis scaled from vertical travel time, i.e., refers to the position in space of an image obtained using a known reference velocity, reduce the computation time and cost. This conversion is often used in exploration geophysics.

Finally, the input $b_1(k_g, k_s, z)$ is used to compute the predicted multiple of equation 1. Once added to b_1, b_{3IM} suppresses all first order internal multiples. It is important to mention that this process does not remove multiples; it just attenuates them (Weglein et. al., 1998).

Equation 1 is partly intuitive and empirical and requires a deep physical and mathematical analysis to understand completely its foundations, but is clear to see that b_1 is a quantity transformed to (k_g, k_s, z) and then is broken into lower-higher-lower contributions. This latest is a key condition in the integral because allows to select the appropriate portion of each odd terms in the series. In terms of the data this means the algorithm discriminates or locates vertically portions of the data that correspond with odds terms in the series.

The main objective of this work is to apply1D version of the inverse scattering series internal multiple attenuation algorithm on 2D land field data. In order to accomplish this goal, we first implemented the algorithm in 1D synthetic data (Hernandez, and Innanen, 2012) and then in 2D marine common offset physical model data (Hernandez, Innanen, and Wong, 2012). Finally, using these two previous experiences we applied in 2D land field data from Northeast of British Columbia, Canada.

SYNTHETIC ANALYSIS OF INTERNAL MULTIPLE PREDICTION

In this section we examine using synthetic data the relationship between the parameter epsilon in the algorithm and aspects of the data, such as wavelet, central frequency, combination of depths and velocities, and noise. The goal is to complete these experiments with a strong intuition for optimal estimation of epsilon in order to move to physical model data and field data.

By knowing or controlling the source wavelet the estimation of the value of this parameter is straightforward. In more complex data, where the source wavelet is uncertain the autocorrelation can be applied to have a sense between what values the parameter epsilon (ϵ) varies.

In the next three examples examine the sensitive of the algorithm to the parameter epsilon, with the expectation that an underestimation or overestimation of epsilon (ϵ) would lead us to a wrong prediction.

Sensitivity to Epsilon

Since the parameter epsilon is related to width of the source wavelet we made a series of tests varying the central frequency of the source wavelet in order to evaluate how sensitive the algorithm is to the parameter epsilon (ϵ). The parameters used to generate the models are given in Table 1. We used this simple model to generate different data set with different values of the central frequency: 120, 80 and 15Hz, and applied different values of epsilon (ϵ).

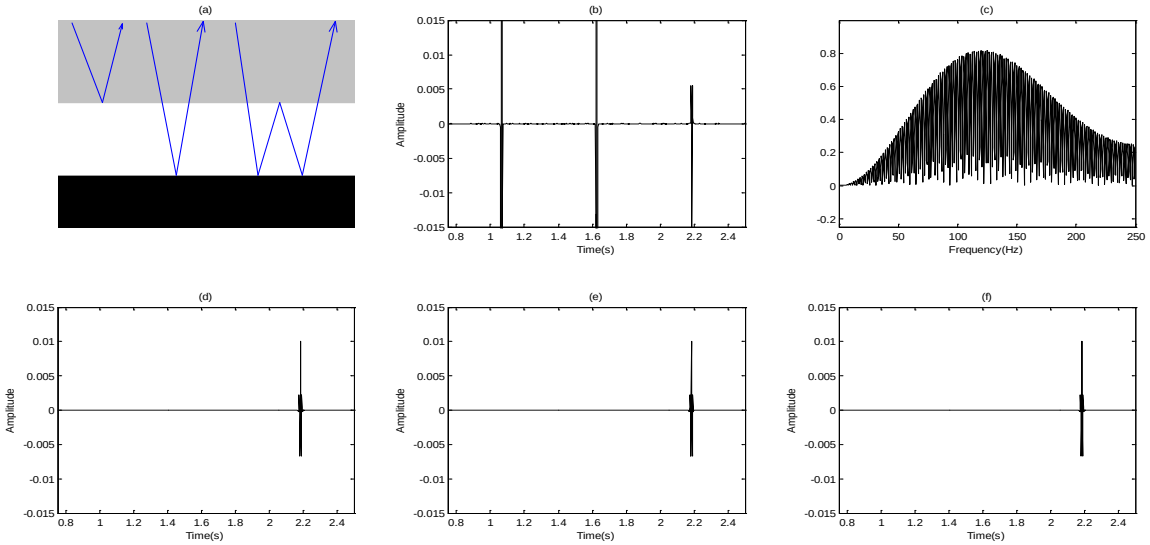

Figure 1: High Frequency experiment: (a) Sketch of the input model. (b) Synthetic medium frequency (120Hz) input data, two reflectors and one internal multiple. (c) Amplitude Spectrum of the synthetic data. (d) Output prediction using a value of epsilon optimum for low frequency 15 Hz (60 samples points). (e) Output prediction using a value of epsilon optimum for high frequency 80Hz (15 samples points). (f) Output prediction using a value of epsilon optimum for high frequency 120Hz (8 samples points).

High Frequency data (120Hz)

In the test, Figure 1, we used a high frequency of 120Hz to generate the data. The values of epsilon (ϵ) utilized were: 60, 15, and 8 samples points, these values correspond to data set of low, medium and high frequency, respectively.

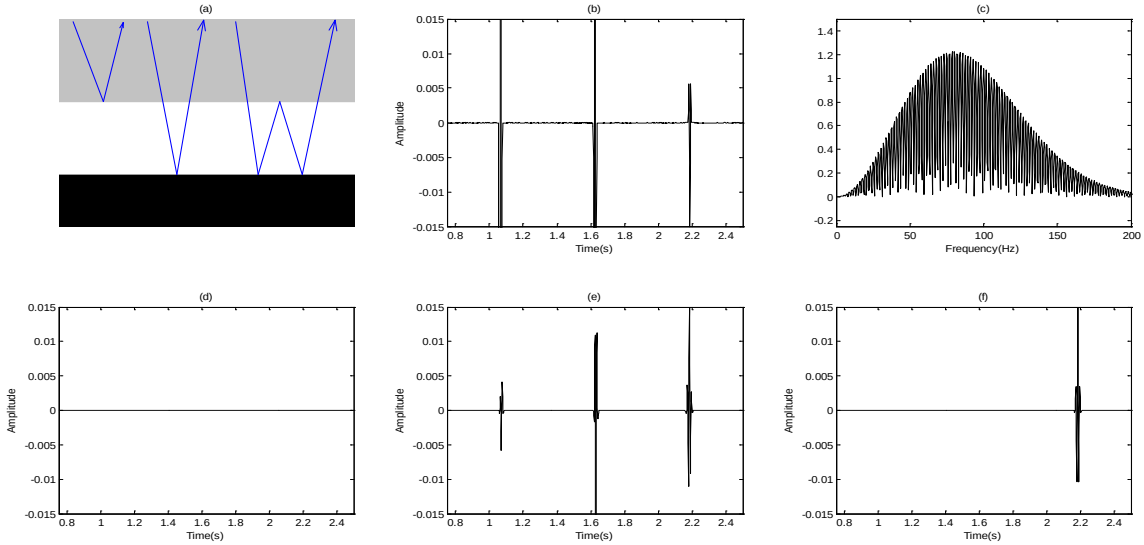

Figure 2: Medium Frequency experiment: (a) Sketch of the input model. (b) Synthetic high frequency (80Hz) input data, two reflectors and one internal multiple. (c) Amplitude Spectrum of the synthetic data. (d) Output prediction using a large value of epsilon, overestimation. (e) Output prediction using a small value of epsilon, underestimation. (f) Output prediction using a value of epsilon optimum for medium frequency 80Hz (15 samples points).

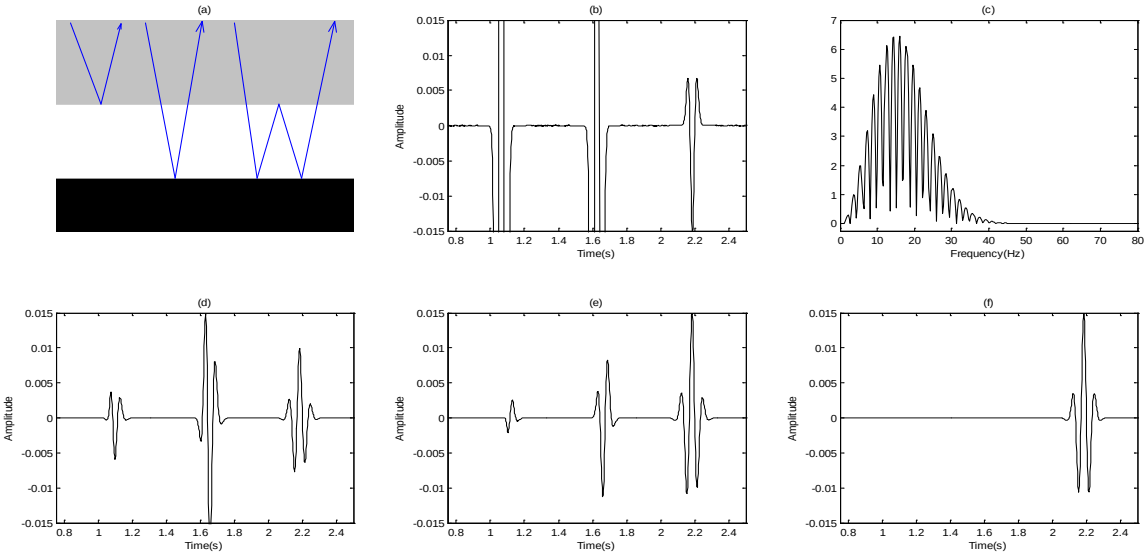

Figure 3: Low Frequency data (15Hz) experiment. a) Sketch of the input model. (b) Synthetic low frequency (15Hz) input data, two reflectors and one internal multiple. (c) Amplitude Spectrum of the synthetic data. (d) Output prediction using a value of epsilon optimum for high frequency. (e) Output prediction using a value of epsilon optimum for medium frequency 80Hz. (f) Output prediction using a value of epsilon optimum for low frequency 15Hz (60 samples points).

Therefore, the correct value for this particular data set is the 8 samples points; see Figure 1, in the bottom of right side. Even though the values of epsilon in the others two cases were wrong or optimum for different frequency value, the results obtained were correct. The algorithm predicted the internal multiple in the three cases at the correct time and similar amplitude. Therefore, based on these results we conclude that for high frequency synthetic data, the algorithm is capable of predict internal multiples using any a value of epsilon as long as is equal or higher than the width of the source wavelet, as we shown in Figure 1.

PARAMETER	VALUE
Sample number	2048
Interval sample time	2ms
Type of wavelet	Ricker
Depths of first interface	800m
Depths of second interface	1500m
Velocity first layer	1500m/s
Velocity second layer	2500m/s

Table 1: Synthetic model parameters, sensitivity of epsilon.

Notice that in this example the smaller value of epsilon is 8 samples points, and is the proper value according to the central frequency of the source wavelet. In the next examples we will show that is an underestimation of the value of epsilon that could lead us a wrong prediction or damaged the data, and that is the case for lower frequencies.

Medium Frequency data (80Hz)

Using the parameters given in Table 1 we generated a synthetic data set with a central frequency of 80Hz. As the previous example the data contain two primaries reflections and an interbed multiple within, in Figure 2 the input data, its amplitude spectrum and the different prediction outputs are shown. In this example for a medium frequency of 80Hz we can notice how a wrong estimation of the parameter epsilon (ϵ) can lead us to a wrong prediction, for an underestimation of epsilon (smaller than width of the source wavelet) can damaged the output significantly, affecting the primaries and/or creating artifacts or wrong events. On the other hand, an extreme overestimation of the parameter epsilon would not damage the output prediction but neither shows any events, because the algorithm is not capable to identify the events.

Low Frequency data (15Hz)

We used the parameters listed in Table 1 and a central frequency of the 15Hz to generate the input data. Notice in Figure 3 that the wavelet is wider comparing to previous examples shown (Frequency 120Hz and 80Hz) as we expected. The proper value of epsilon for a frequency of 15Hz is 60samples points. However, different values of epsilon

were tested to evaluate the results. For values of epsilon for high and medium frequency the algorithm predicted the internal multiple at the correct time but also predicted additional events that damaged the primaries. Therefore, for a low frequency data a wrong estimation, especially an underestimation of the value of epsilon would damage considerably the output prediction.

The importance of the parameter epsilon lies in the fact that events are not delta functions, they have an intrinsic form, the width of the wavelet. The parameter epsilon limits the searching of the subevents that compose the internal multiples. Without the parameter epsilon the algorithm could take one side of the wavelet as a single event and the other side as other events that satisfy a lower-higher-lower pseudo depth condition and construct an internal multiple, but that would be wrong because they are all part of the same event. Therefore, the parameter epsilon does not allow the algorithm to take in account these intra-events. Knowing the wavelet allow us to set in the algorithm what is the minimum width of the events can be seen as single events.

Wavelet Removal

In field data the source wavelet presents the effect of many components, such as source signature, recording filter, surface reflections, and receiver-array response, this components are implicit in the form of the wavelet and its frequency. In synthetic data these components are not present, but still we can remove the effect of the form and frequency of the source wavelet. The wavelet was removed from the original input data; subsequently the new input data takes the form of spikes. We tested three values of epsilon: 8, 15 and 60 samples points using the same input data. The results presented in Figure 4 shows that the algorithm predicted the internal multiples at the correct time and similar amplitude at any value of epsilon, which confirms that epsilon depends on the wavelet; if the data has a spike form the parameter epsilon would not be needed. Moreover, based on this result we can conclude that the response of the algorithm is not affected for the form and/or frequency of the wavelet as long as the parameter epsilon is properly estimated. The parameters used to generate the input data are shown in Table 2.

PARAMETER	VALUE
Sample number	2048
Interval sample time	2ms
Depths of first interface	800m
Depths of second interface	1500m
Velocity first layer	1500m/s
Velocity second layer	2500m/s

Table 2. Parameter of the synthetic model, wavelet removal.

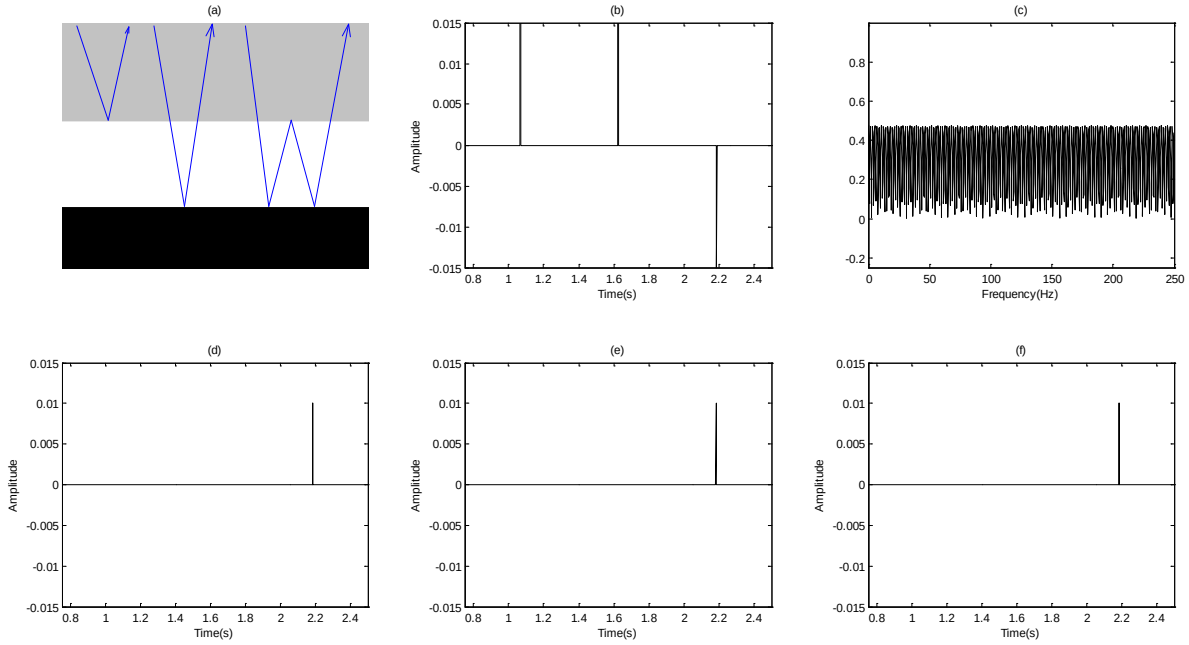

Figure 4: Removal of the wavelet of the input data. (a) Sketch of the model. (b) Synthetic input data, two primary reflections and one internal multiple. (c) Amplitude Spectrum. (d) Output prediction using a value of epsilon equal to 8 samples. (e) Output prediction using a epsilon of 15 samples points. (f) Output prediction using a value of epsilon of 60 samples points.

PARAMETER	VALUE
Sample number	2048
Interval sample time	2ms
Type of wavelet	Ricker
Type of noise	Gaussian
Depths of first interface	800m
Depths of second interface	1500m
Velocity first layer	1500m/s
Velocity second layer	2600m/s
Velocity second layer	4200m/s

Table 3. Parameter of the synthetic model, wavelet removal.

Noisy data

In this experiment we generated noisy synthetic input data to evaluate how the prediction is affected for noise. The noise included in the data was statistical Gaussian noise. The model consists of two primaries and one interbed multiples. The parameters utilized to generate the model are given in Table 3. In the first model there is high contrast of

impedance at second interface (1500m). Consequently, the respective first order interbed multiple would have high amplitude. Three frequencies were used: 30, 70, and 100Hz to generate the input data with additional noise. Appropriate epsilon values were used according to the frequency of the input data: 60, 12, and 5 samples points. In Figure 5 the inputs and outputs prediction are shown. Notice that in the three cases the internal multiples cannot be differentiate from the noise, but in the outputs data the internal multiple is clearly seen.

However, the outputs predictions show a strong event at 1.75s that is the interbed multiple included in the input data. In Figure 6 we show the similar experiment but the model present only a variation in the velocity of the second layer; in this case the impedance contrast is less. The whole parameters are shown in Table 4. The amount of noise, values of frequencies and epsilon used were the same as the fore example. Notice that neither the inputs and outputs predictions show clearly the internal multiple present in the data. In this case the algorithm does not work satisfactory.

Based on the this results we can conclude that if the internal multiple has a strong amplitude the algorithms works correctly even though in the presence of noise, but if the internal multiple has a small amplitude and high amount of noise the results would not be accurate.

PARAMETER	VALUE
Sample number	2048
Interval sample time	2ms
Type of wavelet	Ricker
Type of noise	Gaussian
Depths of first interface	800m
Depths of second interface	1500m
Velocity first layer	1500m/s
Velocity second layer	2600m/s
Velocity second layer	3200m/s

Table 4: Parameter of the synthetic model, noisy synthetic data.

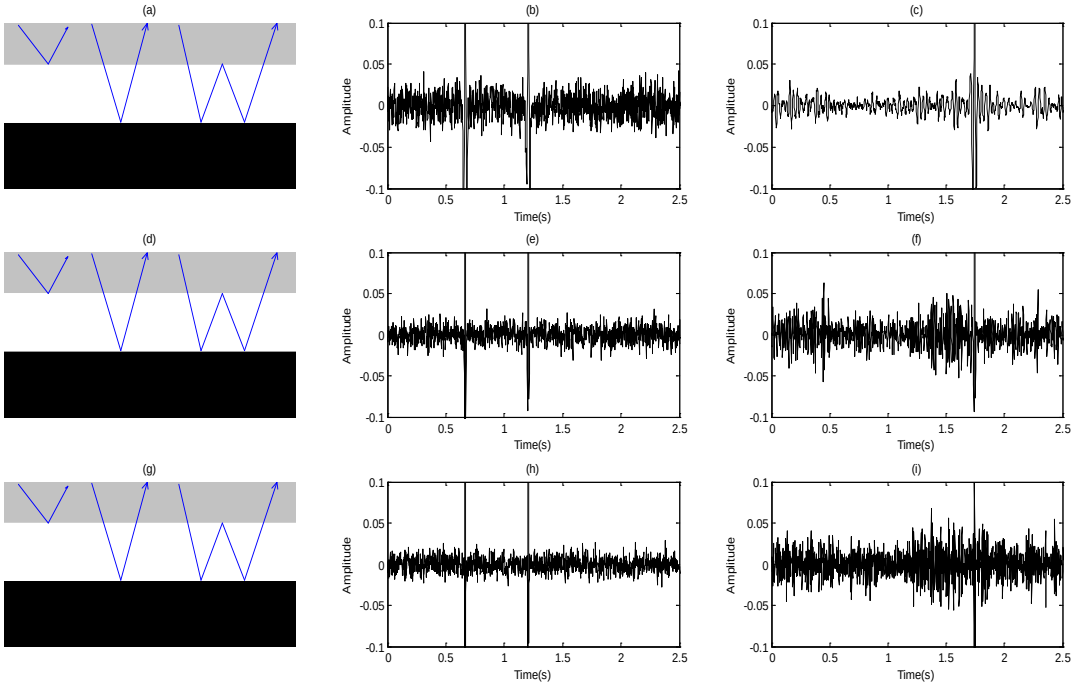

Figure 5: High impedance contrast model with Gaussian noise. a) Sketch of the model, b) Synthetic low frequency (30Hz) input data, c) Output prediction, epsilon 60samples points, d) Sketch of the model, e) Synthetic medium frequency (70Hz) input data, f) Output prediction, epsilon 12 samples points, g) Sketch of the model, h) Synthetic high frequency (100Hz) input data, i) Output prediction, epsilon 5 samples points.

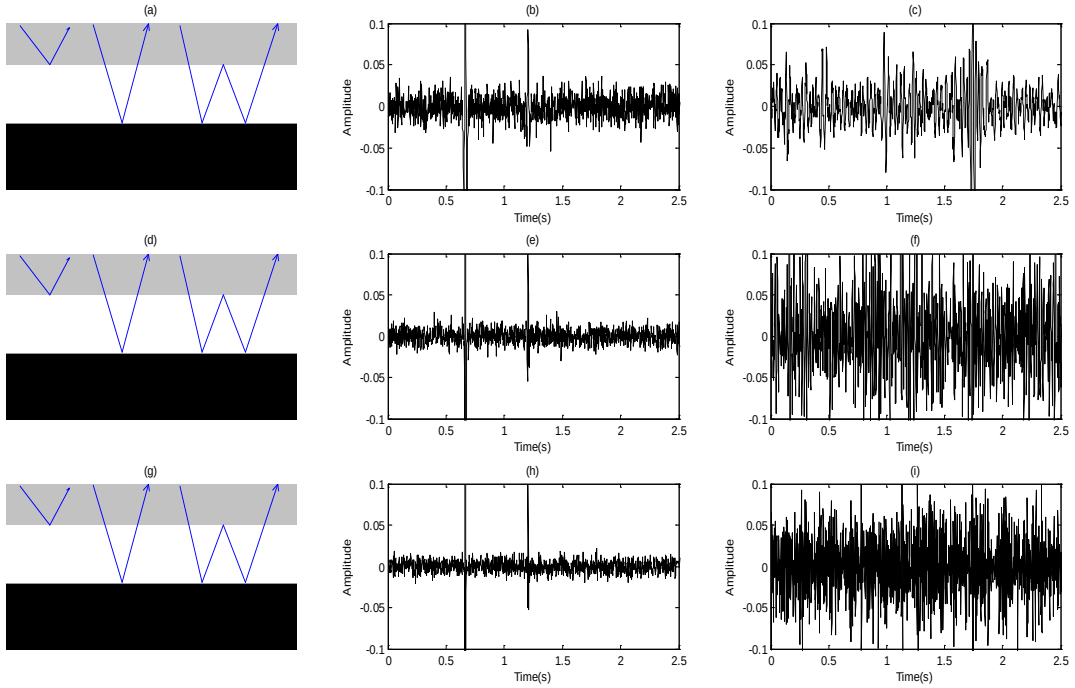

Figure 6: Low impedance contrast model with Gaussian noise. a) Sketch of the model, b) Synthetic low frequency (30Hz) input data, c) Output prediction, epsilon 60samples points, d) Sketch of the model, e) Synthetic medium frequency (70Hz) input data, f) Output prediction, epsilon 12 samples points, g) Sketch of the model, h) Synthetic high frequency (100Hz) input data, i) Output prediction, epsilon 5 samples points.

APPLICATION ON PHYSICAL MODELLING LAB DATA

We conducted a 2D common-offset seismic survey over the model shown in Figure 7, with 401 traces at a spacing of 10m (field scale). The source and the receiver were slightly immersed in the water. The frequencies emitted varying between 5 to 100Hz (field scaled) (Hrabi, 1994).

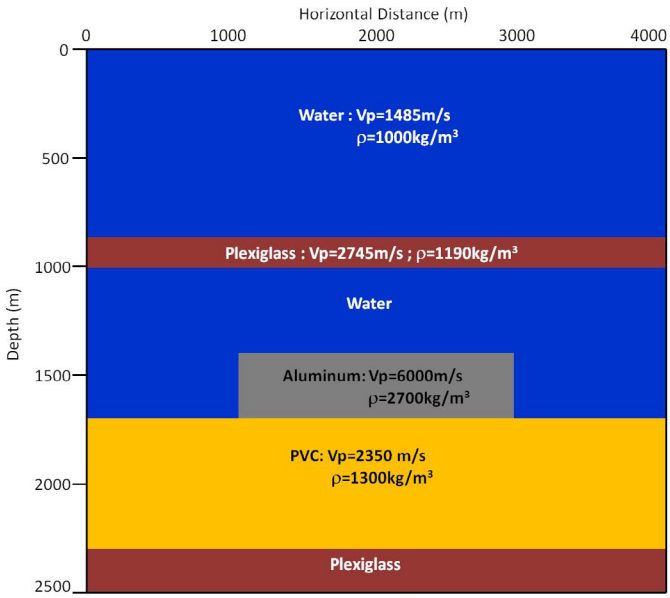

Figure 7: Schematic diagram of the model used

The model used in this study consisted of a PVC slab, Plexiglass, smaller Aluminum slab, Plexiglass immerse in Water, Figure 7 shows sketch of this model and its physical characteristics. The scaling used for distance in the model was 1:10000, therefore, 1cm long by 2.5cm deep model represented 100m in horizontal distance and 250m in depth.

The processing flow implemented for this data set is listed in Table 5. The dominant frequency is 35Hz. The data in general is high quality, not noisy and the reflections are well defined in the entire section. Figure 8 shows the seismic data set after processing. This data set is the input of the algorithm.

STANDARD FLOW
Deconvolution
Velocity analysis
Statics (No surface consistent)
Noise Attenuation filter

Table 5. Processing work flow

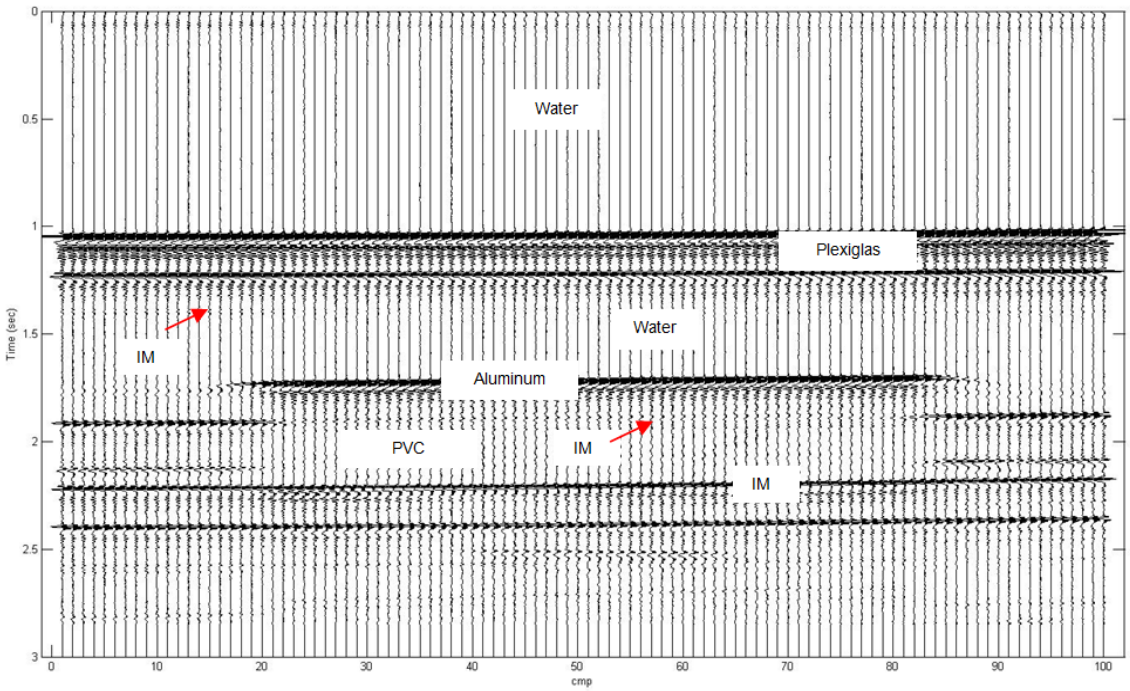

Figure 8. Common-offset gather: after processing

Estimation of epsilon

Autocorrelation is a very useful mathematical tool for finding repeating patterns, such as the existence of a periodic signal which has been buried under noise, and/or identifying the missing fundamental frequency in a signal implied by its harmonic frequencies. Autocorrelation is frequently used in seismic processing to designing the deconvolution operator. In this work, the autocorrelation is used to estimate the source wavelet in subsequently a value of parameter epsilon (ϵ). Figure 9 shows the autocorrelation of input data.

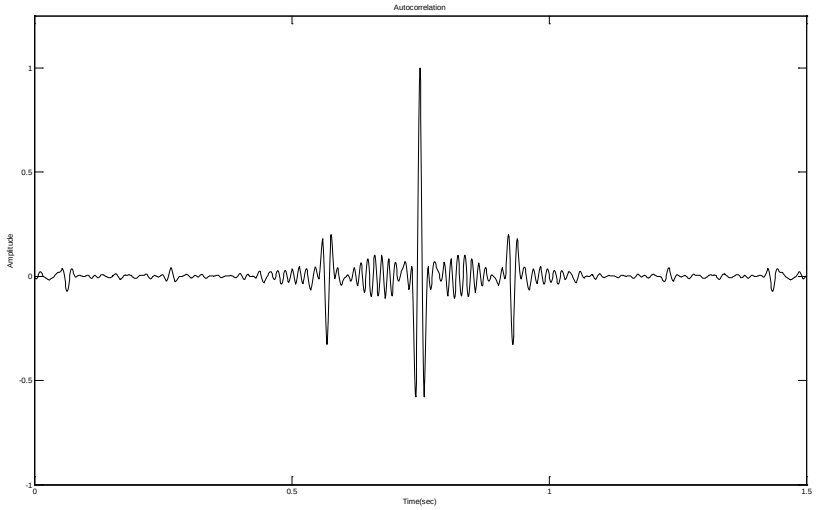

Figure 9. Autocorrelation of the physical model data.

Results

We applied our 1D multiple attenuation algorithm on physical model data and the results are quite satisfactory. The prediction is showed in Figure 10. Setting at epsilon (ϵ) value of 50 (sample points) we predicted internal multiples reflections at 1.4, 1.9, 2.3, 2.6 and 2.7 seconds as we expected according to the model. The ray path of the main first order internal multiples are shown in Figure 11. The form of the wavelet is affecting the output prediction. Notice in Figures 10 and 11 that the strongest internal multiples is IM3 (1.83s) due to the high contrast of impedance between the aluminum layer and water, is very strong in the input data and output prediction. Moreover, the output prediction presents reverberations or ringing effect. A certain amount of seismic energy is not been transmitted from one layer to the next through the water and aluminium layers. It remains trapped within of these layers producing additional arrivals on the section at each rebound.

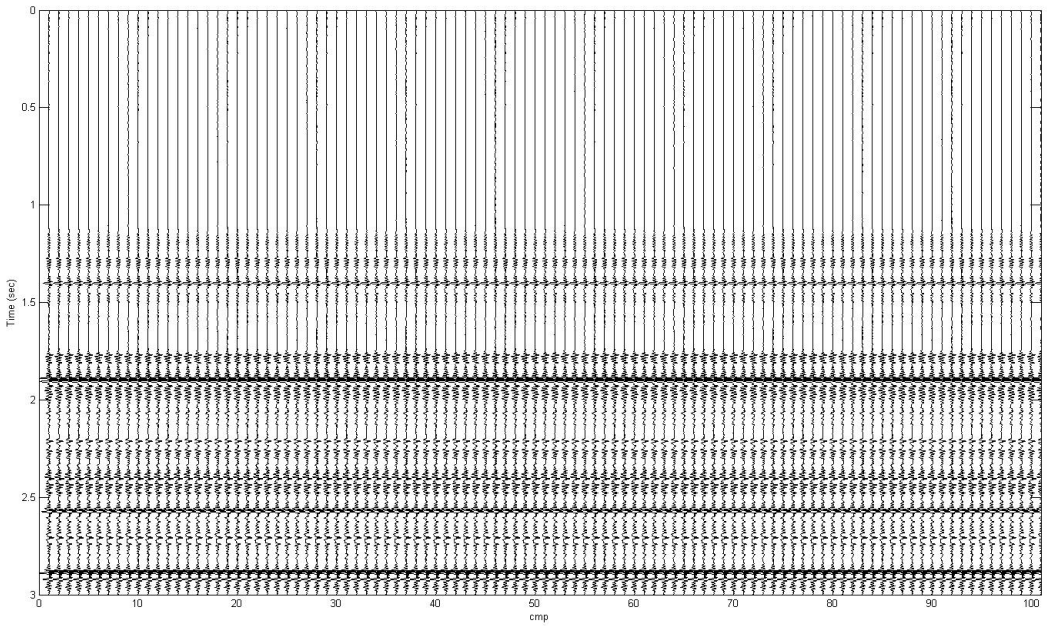

Figure 10. Output prediction, stack section full of internal multiples.

ZERO OFFSET INTERNAL MULTIPLE PREDICTION ON LAND DATA

For the exploration of oil and gas reservoirs, multiples can be one of the main issues in applying the seismic method. In this section we will present the methodology and results of the application of the algorithm on land field data. Two experiments will be explain: 1) synthetic data test, using well log information (velocity and density logs), and 2) field data test, performed on 2D land seismic data. Both data sets were donated by Nexen Inc., and belong to the northeastern of British Columbia (NEBC). Although both data sets are in the same area, the well does not intercept the 2D seismic line; in fact this well is 5km away from the seismic line. For this reason, we excluded some geological intervals of the synthetic model that are present in the well log information but no in the seismic line,

such as: Bucking Horse, Spirit River, Tetcho, Muskwa and Evie, in order to compare the well markers with major seismic reflections and their corresponding internal multiples.

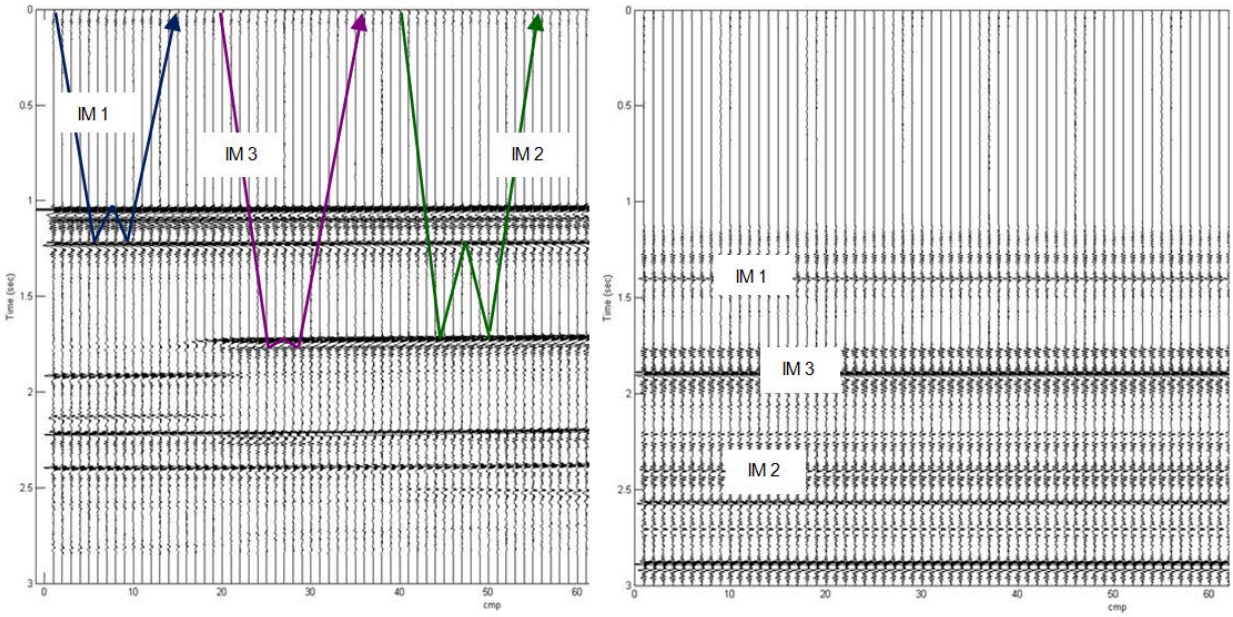

Figure 11. Comparison between input data (left side) and output prediction (right side).

Geological Background of the major reflectors

The 2D line used in this work was acquired in northeast of British Columbia (NEBC). The surface of the area is mostly tills rich in clay and sediments of origin glaciolacustrine. The area presents in some places thick organic deposits in poorly drained areas (Levson et. al. 2005). In the next sections, we will describe briefly the geological characteristics of the formations that are present in the 2D seismic line, see Figure 5.2, these formations are named: Banff, Exshaw, Jean Marie and Otter Park. Moreover, well log information of the area was available and used for identification of which surfaces were generating internal multiples due to high contrast of impedance and also for the construction of the synthetic model of the area.

Banff Formation

The Banff Formation belongs to the Fort St Jonh Group (Lower to Mid Cretaceous), in particular Banff Formation is the age Missisipian. This formation consist of shales and marlstones, bedded chert and carbonates towards the east and the surface. The thickness of the formation in this area is around 140m. The Fort St. John Group was deposited in a marine environment. The shallower part of this formation is a sequence of interbedded sandstones, siltstones, and shales (Glass, 1997). In the well log, Figure 5.3, the Banff formation exhibits high frequency variations in velocity and density logs. In the seismic section, Figure 5.2, this reflector is found around 0.52s.

Exshaw Formation

The Exshaw Formation consists of black shale in the lower part, and siltstone and limestone in the upper part. It has a thickness of 45 metres approximately. Its age is Missisipian as well. The Exshaw Formation is unconformably overlain by the Banff Formation. In the well log there is an abrupt increment of the velocity (~5550 m/s) that start at the top of the formation that also corresponds to low values in the GR. The density log is quite uniform; values are around 2700kg/m^3, except for two picks at 820 and 860m (TVD) of unknown genesis, Figure 12.

Jean Marie Formation

The Jean Marie Formation is a member of The Redknife Formation of Frasnian age (Upper Devonian), is composed of argillaceous, silty and dolomitic fossiliferous limestone. The P-wave shows a strong velocity pick of 5250m/s in the interface Exshaw-Jean Marie, but rapidly chance to a uniform tendency with an average velocity of 3450m/s. This formation exhibits high frequency variations in density, Figure 12.

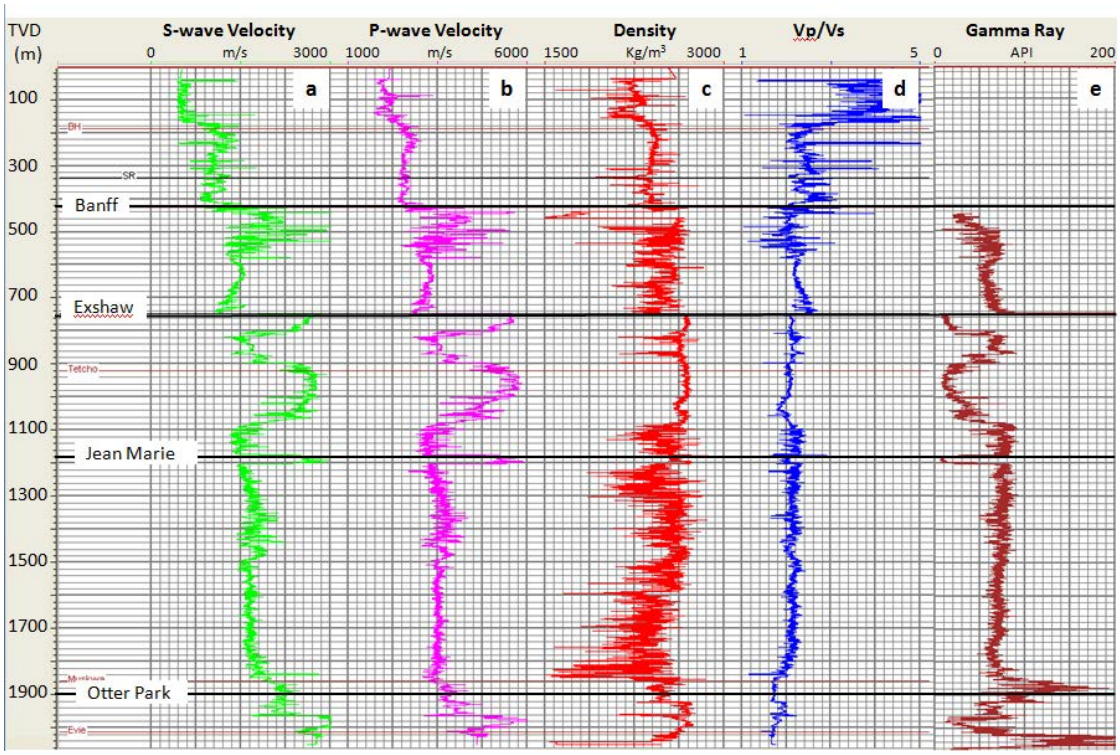

Figure 12: Well log from the area: a) S-wave velocity log, b) P-wave velocity log, c) Density log, d) Vp/Vs, e) Gamma Ray. Modified from Zuleta (2012).

Otter Formation

The Otter Park Formation is composed by medium to dark grey calcareous shale of Givetian age (Middle Devonian). This formation also present radioactive siliceous black shale beds (McPhail et al., 2008; BC Ministry of Energy and Mines, 2011). This shale has a thickness of 270m towards the southeast of the Horn River Basin and thins to the

north and west. This formation was originated from deposits of clays, fine siliceous (silica-rich) muds, and organic matter, in the deeper, poorly oxygenated waters. Otter Park has increase of velocity in the P-wave log and a decrease Gamma Ray in the deeper part of the formation due to the presence of organic lean argillaceous carbonates, see Figure 12.

According to geological information and well logs we expected a high impedance contrast between the source-receiver medium and Banff Formation, and Jean Marie and Otter Park reflectors because a high velocity values. These high impedance contrasts can potentially causes the generation of internal multiples bouncing between these reflectors or the combination of them.

PARAMETER	VALUE
Sample number	2048
Interval sample time	2ms
Velocity and depth of the first interface	3140m/s at 420m
Velocity and depth of the first interface	3900m/s at 750m
Velocity and depth of the third interface	3450m/ s at 1180m
Velocity and depth of the fourth interface	5250m/s at 1900m
Epsilon	13
Type of wavelet	Ricker
Wavelet central frequency	80Hz
Wave speed of the source/receiver medium	1500m/s

Table 6: Parameter used to generate the synthetic model of the NEBC.

Synthetic Model of the field data

Well log information of the area is shown in Figure 5.3. This information allowed us to generate a synthetic seismogram, convolving the reflectivity obtained from well logs with a Ricker wavelet. The well log information represents a regional scenario of the area.
The main objective in generating a synthetic seismogram using well log information is to predict the seismic response of the area, and to evaluate how the algorithm works in this geological setting, and predict internal multiples based on the combination of subevents, only considering primaries, and then compare the results of the field data in terms of time and amplitudes. We also used this model to pre-evaluate the value of the parameter epsilon (ϵ), and use it as reference in the field data test.

In order to simplify the synthetic model the following formations were excluded: Bucking Horse, Spirit Horse, Tetcho, Muskwa and Evie. Details of the parameter used for the synthetic model are show in Table 6.

Figure 13 shows the input synthetic data, this section contain four primary reflections at 0.56s (Banff), 0.77s (Exshaw), 1.0s (Jean Marie), and 1.41s (Otter Park), and three first orders internal multiples around 1.0, 1.21s, and 1.83s. The output prediction is shown in Figure 13, in this figure internal multiples are found at 1.0s, 1.2s, 1.4s, 1.65s, 1.83s, 2.0s and 2.3s The value of epsilon (ϵ) used was 13 sample points.

The first order internal multiple due to the high impedance contrast between Banff and the receiver/source medium arrives at 1.0s, coinciding with the Jean Marie reflector. The strongest internal multiples arrives at 1.6s, is a short-path multiple its amplitude is large due to high contrast of impedance between Jean Marie and Otter Park. This high contrast of impedance between those interfaces is also generating a strong long-path multiple that arrives at 1.83s, see Figure 13.

Field data application

The 2D multicomponent land seismic field data set used was provided by Nexen Inc., in this work we only used the P wave. The data itself is high quality (high S/N ratio), and conveniently present internal multiples that are interfering and masking the primary reflections. The source used to acquire this data set was vibroseis, interval sample time of 2ms, receiver interval of 10m, and sources were found every 60m. Sensor Geophysical processed the data, and the processing sequence is presented in the following table. In addition, the first 250ms of this data set was muted because contained noise. Figure 14 shows the field data after processing and muting; this data was used as input data.

Conventionally, seismic multiples are removed prior to stacking, in this work we applied the 1D internal multiple attenuation algorithm after the data was stacked for two reasons: 1) since the algorithm works in a 1D medium the input data must be as close as possible to a normal incidence trace, in a flat area an stacked trace is taken to be the response of a normal-incidence reflection at the common midpoint (CMP), besides the staking process remove the effect of the geometry, and 2) the algorithm is very sensitive to noise or other artefacts that are attenuate with the stacking process.

As it was mentioned in previous chapters one of the most important parameters in this technique is the parameter epsilon (ϵ), in order to estimate the value of it an autocorrelation of one trace was performed, see Figure 15. Besides, the results of the synthetic model of NEBC also provided a sense of the range that epsilon could be. In Figure 16 a comparison between the input synthetic section and input field data is shown. The models are very similar which later allow us to compare the outputs prediction and the arrival times of the internal multiples, Figure 18.

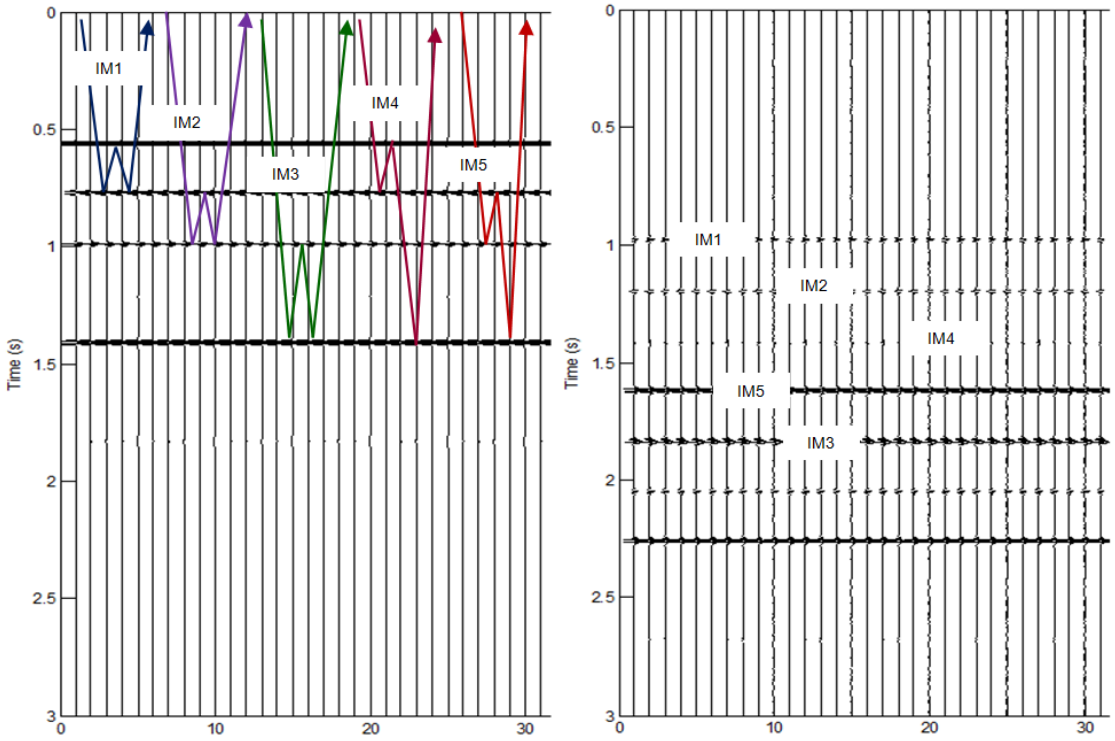

Figure 13.Comparison of synthetic model data of the NEBC (left side) and synthetic output prediction (right side).

In Figure 17 a prediction output stacked section is shown. Notice this section only contain multiples and noise, but no reflections. The stronger internal multiples arrive around: 1.0s, 1.25s, 1.6s, 1.8s, 1.9s, and 2.1s. The value of epsilon that achieved this prediction was 20 sample points. Figure 18 shows a comparison of the output prediction of the synthetic model and the output prediction of the field data. These two sections point out where the internal multiples could be found. The output prediction present certain amount of noise, however the internal multiples are identified clearly.

Figure 19 shows a comparison between the input field data and the prediction output, is a zoom of the central part of both sections. Notice that between 0.9s and 1.4s the algorithm predicted the internal multiples that are present in the input data, the times are the same but the amplitude are slightly different. This output prediction section can be considered a map of the places where the internal multiples can be found. Besides, using this technique the analyst can verify if an interbed multiple is interfering with a primary and affecting the amplitude of it, like we shown in this chapter. This is very important result because an erroneous value of the amplitude can be very harmful mistake in the application of specialized characterization techniques such as AVO.

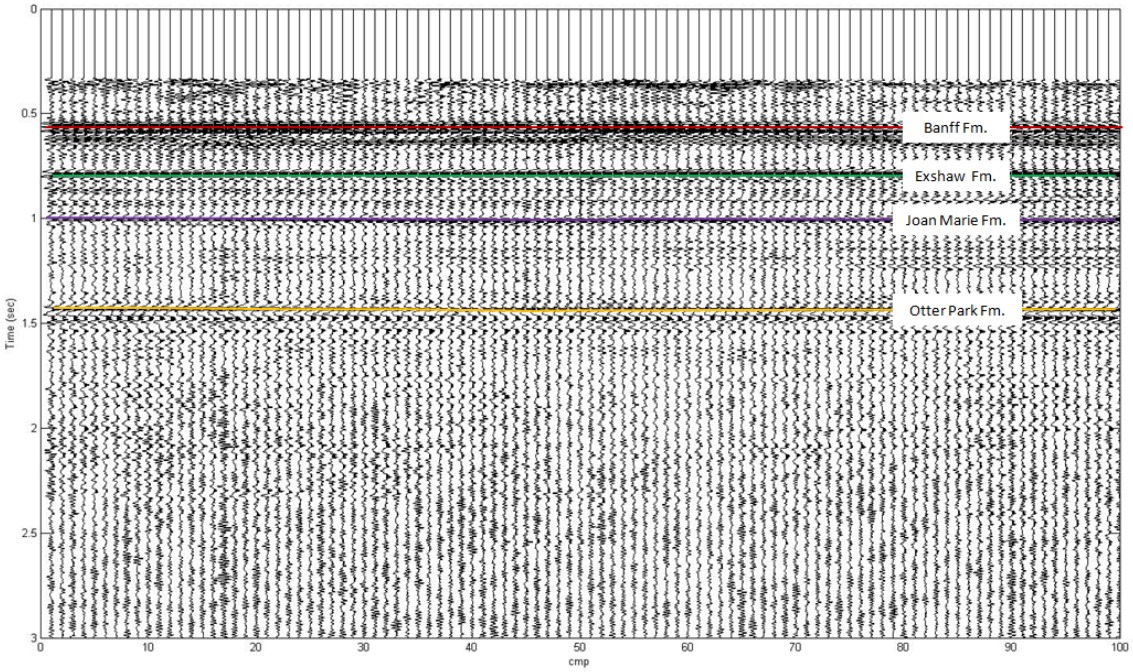

Figure 14. Zero offset field data used as input. This section is shows the major geological markers.

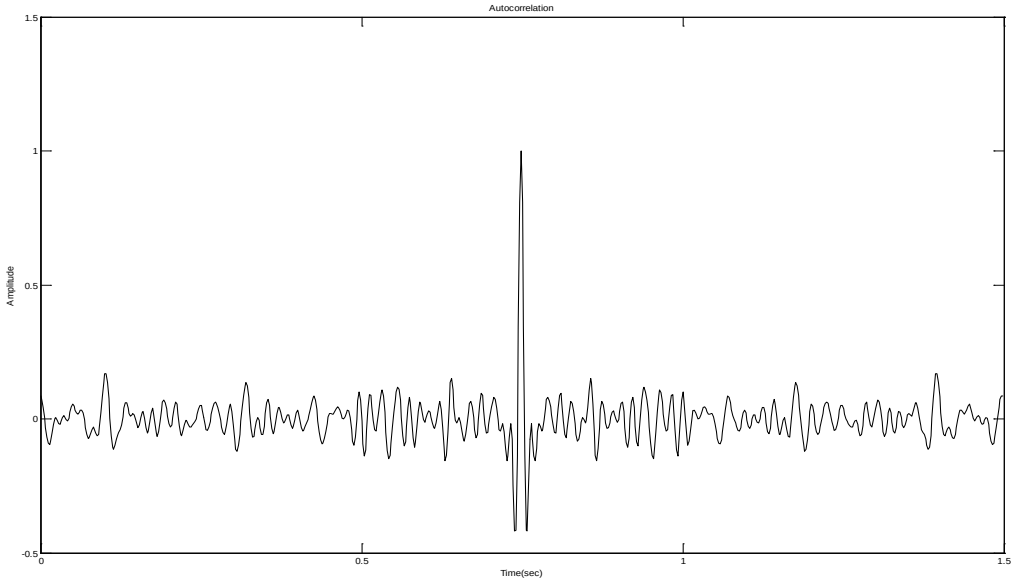

Figure 15.Autocorrelation of the input data.

Processing sequence
Geometry assignment, trace edits and kills
H1/H2 Rotation: 20 degrees.
Amplitude recovery: Spherical divergence correction
Singular Value decomposition (SVD) filter to remove ground roll
FK filter to remove surface generated noise
Surface-consistent deconvolution (Spiking)
Prewhitening
Vibroseis Decon compensation
Refraction static corrections, Datum 600 m, Vremp =2200 m/s
Surface-consistent Statics
Surface-consistent Amplitude scaling
T – F Adaptive Noise Suppression, Offset consistent Gain Control
TV Spectral whitening
Normal moveout correction. Front end mute. Automatic gain control
CDP stack
TV Spectral whitening
FK filter to remove surface generated noise
Trace equalization. F-X Filtering. Diffusion filter
FD Time migration. Band pass filter
Trace equalization
Time variant scaling: mean, centre-to-centre, multiple gates

Table 6. Processing work flow.

As we expected according to the synthetic model of the area, in the output field data prediction there is a first order internal multiple due to the high impedance contrast between Banff and the receiver/source medium that arrives around 1.0s, coinciding with the Jean Marie reflector. Moreover, we identified a strong internal multiples arriving around 1.6s, this is a short-path multiple, its amplitude is large due to high contrast of impedance between Jean Marie and Otter Park. This high contrast of impedance between those interfaces is also generating a strong long-path multiple arriving at 1.83s.

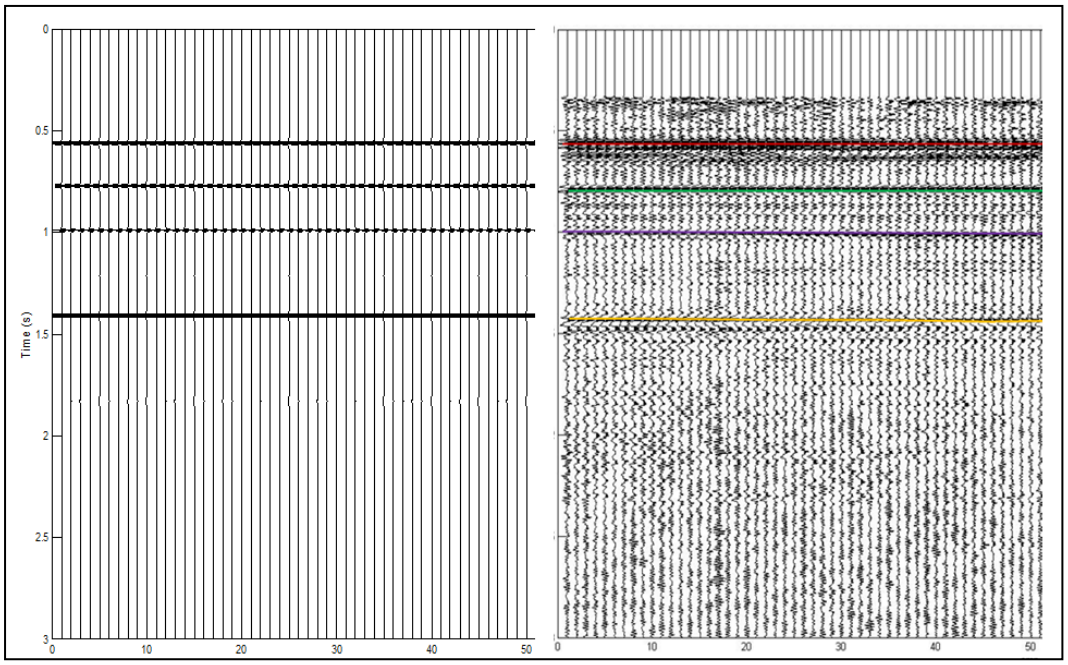

Figure 16.Comparison of synthetic model data (left side) and input field data (right side) of the NEBC.

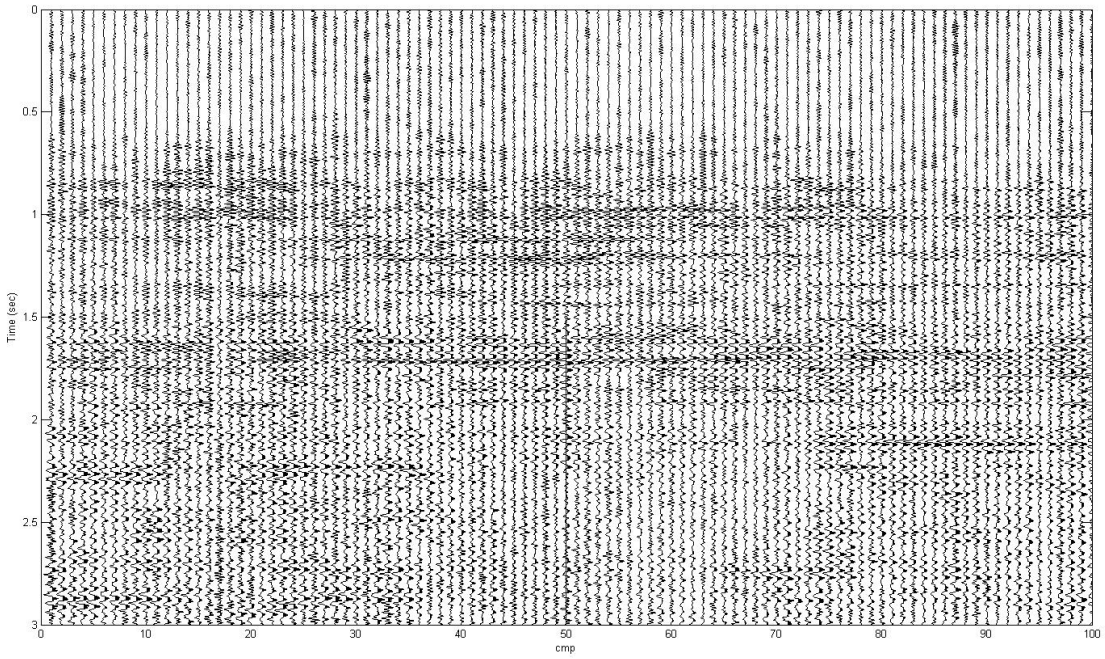

Figure 17.Output prediction, stack section.

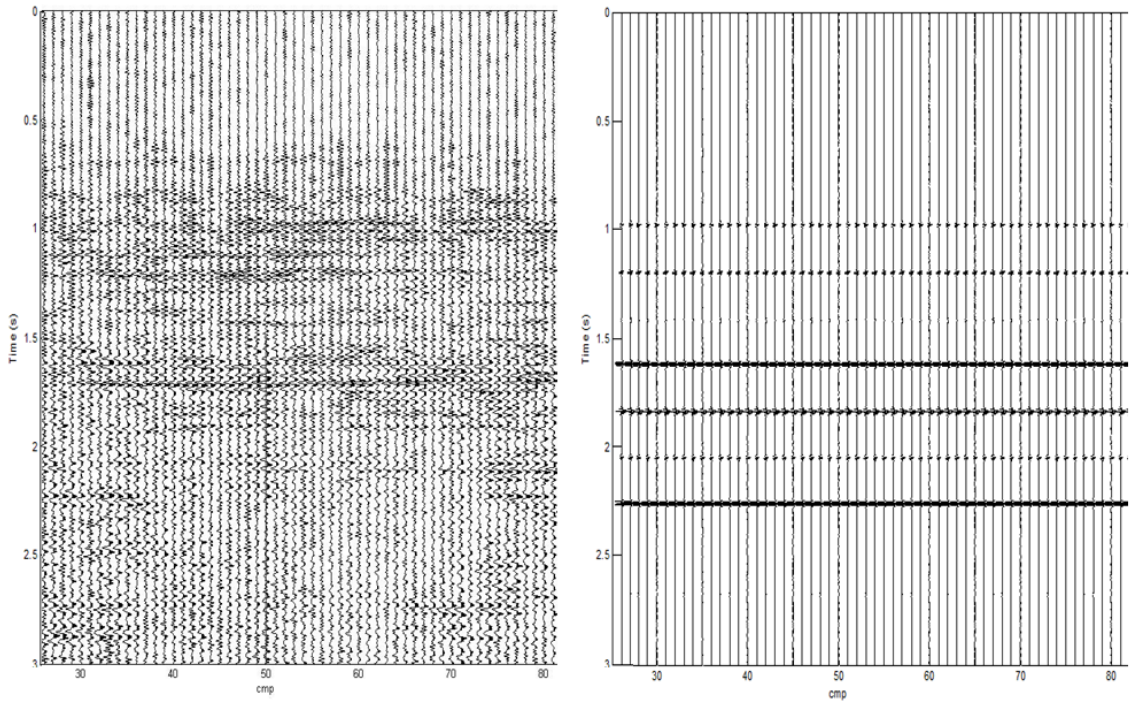

Figure 18.Comparison of output prediction of the field data (left side) and output prediction of the synthetic data (right side) of the NEBC.

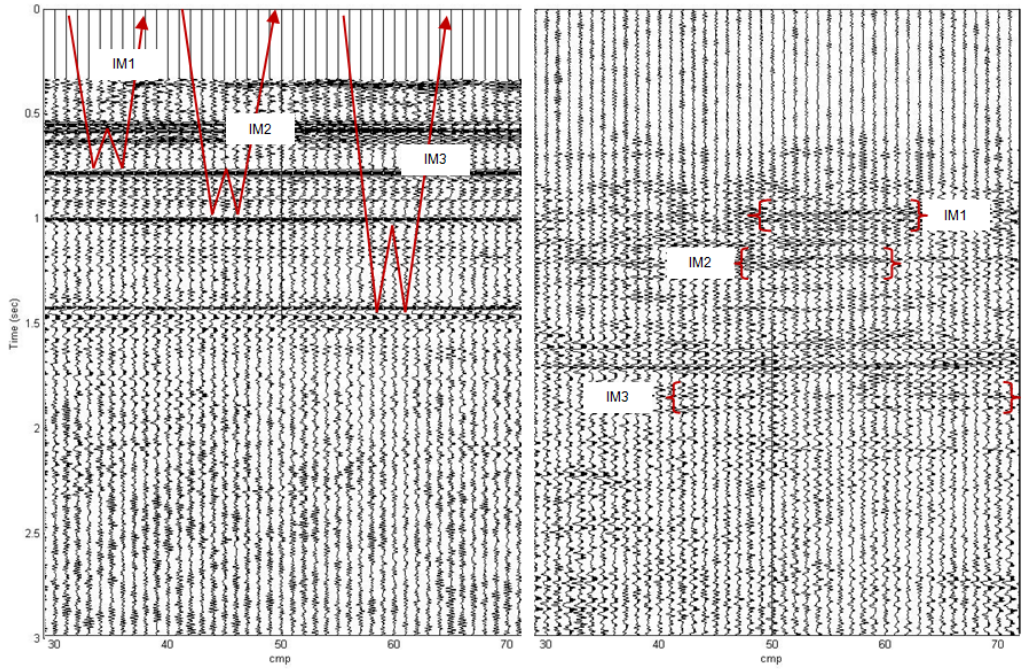

Figure 19.Comparison between input data (left side) and output prediction (right side), field data.

CONCLUSIONS

The principal objective of this work was to apply and test an inverse scattering internal multiple attenuation algorithm based on the work of Weglein and Araujo (1998). This work shows that the algorithm is capable to attenuate internal multiples without any a priori information about the medium through which the waves propagate.

Based on the synthetic experiments we can conclude that for smaller epsilon values, the algorithm affects the primaries. Therefore, an underestimation of epsilon could damage significantly important information present in the data. An overestimation of the value of epsilon would not damage the data, but the output will not show any internal multiples or other seismic events. The components of the wavelet do not affect the prediction of internal multiples using this technique as long as the parameter epsilon is well estimated. The algorithm works satisfactory in noisy synthetic data with noise if there is a high contrast of impedance at the bottom reflectors that generate the internal multiple. The algorithm does not show accurate results in noisy data if the internal multiple has small amplitude.

We conducted 2D marine common offset seismic survey in the physical model lab of the University of Calgary. We used the physical model data acquired in a controlled environment with certain quantity of noise to test the algorithm. There is also a high contrast of impedance between materials. The results found indicate that the algorithm predicted multiples at the correct time and similar amplitudes in a high quality data, without any a priori information about the subsurface. Autocorrelation of the input data is recommended to estimate the value of epsilon. Pre-processing of the data is required. The output prediction depends strongly on the parameter epsilon. The value of epsilon (ϵ) that performed the best prediction was 50 (sample points). The input data and output prediction presents reverberations or ringing effect. A certain amount of seismic energy is not been transmitted from one layer to the next through the water and aluminium layers. It remains trapped within of these layers producing additional arrivals on the section at each rebound. The algorithm is capable of predicts these reverberations.

The experience and knowledge acquired with the application of the algorithm on synthetic data and then physical modeling data allowed us to finally apply the internal multiple attenuation algorithm on field data. The 2D seismic data is high quality, presents strong reflections, low noise, and some internal multiples. Since we are running a 1D version of the algorithm, the input data has been stacked, and muted in order to be as free as possible of noise, because the algorithm is very sensitive to noise. The input section contains primary reflections at 0.6s, 0.8s, 1.0s, and 1.43s. The output prediction presents noise, however, the internal multiples are identified clearly around 1.0s, 1.25s, 1.6s, 1.8s, 1.9s, and 2.1s. The value of epsilon (ϵ) used was 20 sample points.

Using this technique the analyst can verify if an interbed multiple is interfering with a primary and affecting the amplitude of it. This is very important result because an erroneous value of the amplitude can be very harmful mistake in the application of

specialized characterization techniques such as AVO. This output prediction section can be considered a map of the places where the internal multiples can be found.

For future work we recommend the application of adaptive subtraction method to remove the predicted internal multiples from the input data by estimating shaping filters, minimizing the difference or misfit between the input data and the output prediction using least-squares. Moreover, we recommend the application of the algorithm on geological complex seismic data, and developing of a 2D version of the algorithm.

ACKNOWLEDGEMENTS

We thank the sponsors of CREWES for their crucial financial support. Thank to Dr. Donald Lawton and Dr. Joe Wong for their suggestions and comments. Special thanks to Nexen Inc. for donated the well and seismic data.

REFERENCES

Araujo, F.V., Weglein, A.B., Carvalho, P.M., and Stolt, R. H., 1994, Inverse Scattering series for multiple attenuation: an example with surface and internal multiple: 64th Annual Meeting of the Society of Exploration Geophysics, Expanded Abstracts, 1039-1041.

Hernandez, M., Innanen, K., and Wong, J., 2011, Internal Multiple Attenuation based on inverse scattering: Theoretical review and implementation in synthetic data. CREWES Research Report. Volume 23.

Hernandez, M., Innanen, K., and Wong, J., 2011, Internal Multiple Attenuation based on inverse scattering: Implementation in physical model seismic data. CREWES Research Report. Volume 23.

Weglein, A. B., and Matson, K. H., 1998, Inverse scattering internal multiple attenuation: analytic example and subevent interpretation: Part of SPIE Conference on Mathematical Methods in Geophysical Imaging V, 3453.